

Second-order Wagner theory for two-dimensional water-entry problems at small deadrise angles

By J. M. OLIVER

School of Mathematical Sciences, University of Nottingham, Nottingham NG7 2RD, UK

(Received 19 May 2006 and in revised form 24 May 2006)

The theory of Wagner from 1932 for the normal symmetric impact of a two-dimensional body of small deadrise angle on a half-space of ideal and incompressible liquid is extended to derive the second-order corrections for the locations of the higher-pressure jet-root regions and for the upward force on the impactor using a systematic matched-asymptotic analysis. The second-order predictions for the upward force on an entering wedge and parabola are compared with numerical and experimental data, respectively, and it is concluded that a significant improvement in the predictive capability of Wagner's theory is afforded by proceeding to second order.

1. Introduction

The dynamics of high-velocity water entry is of practical importance in numerous applications ranging in scale from droplet motion to asteroid impact. As described in the reviews of Faltinsen (1990), Korobkin (1996), Korobkin & Pukhnachov (1988) and Mizoguchi & Tanizawa (1996), for example, the most well-studied scenario is the slamming of the fore-body of a ship on the sea surface, which can cause localized and eventually catastrophic damage to the hull. The accurate prediction of the pressure distribution and force on an impactor is therefore of significant importance to ship design, which is the practical motivation for this paper.

Even in the simplest two-dimensional water-entry problem in which the flow starts from rest and the effects of viscosity, compressibility, gravity, surface tension and air cushioning are neglected, the nonlinearities involved in the locations of, and boundary conditions on, the impactor and free surface have hampered severely the mathematical analysis. The only exact analytic results are for the self-similar flow of a wedge entering a liquid half-space, which was first studied by Dobrovolskaya (1969). More recently Fraenkel & Keady (2004) proved that the supremum of the contact angle between the free surface and the wedge is strictly less than $\pi/4$ for all vertex angles in the open interval $(0, \pi)$, as well as developing an 'all-purpose' integral equation formulation that allowed for the first time numerical computation of the singular limits of small vertex angle, of the contact angle tending to its supremum and of small contact angle. The last of these limits corresponds to the large-vertex-angle regime in which the vectors normal to the impacting body and to the undisturbed free surface are nearly parallel. The main thrust of theoretical efforts has focused on the simplifications afforded by this 'small deadrise angle' regime based on those used in the pioneering work of von Kármán (1929) and Wagner (1932) on the alighting of seaplanes. The theory is applicable during a small initial time interval to the

impact of an arbitrary blunt body and has the following structure. In an outer region comparable in size to the extent of the impactor below the undisturbed waterline the bulk flow is at leading order as if the liquid were being loaded by an expanding flat plate, with the boundary conditions being linearized and imposed on the initial position of the free surface. This description breaks down at the ends of the plate in inner regions a factor of the deadrise angle squared smaller than the outer one, where the nonlinear terms in the Bernoulli condition come into play and force the free surfaces to ‘turn over’ in small high-pressure jet-root regions on the body, ejecting thereby thin, rapidly moving splash jets. A key observation of Wagner (1932) was that at leading order the perturbed free surface must rise up to meet the impacting body at the ends of the plate. These so-called ‘Wagner conditions’ determine the extent of the expanding flat plate, and hence the subset of the contact region over which the pressure is appreciable. Although Wagner’s ideas have been justified formally using matched-asymptotic expansions in the studies of, for example, Cointe & Armand (1987), Wilson (1989), Cointe (1989), Howison, Ockendon & Wilson (1991) and Oliver (2002), it is somewhat disappointing that in the majority of applications the leading-order theory predicts values for the upward force on the impactor that are significantly higher than the measured ones.

Korobkin (2004) describes in detail the numerous strategies that have been proposed to improve the accuracy of Wagner’s theory, and to extend thereby its domain of validity from small deadrise angles (in the range 5° – 15°) to moderate ones (in the range 15° – 30°).† For example, in Logvinovich (1969), Vorus (1996), Zhao, Faltinsen & Aarsnes (1996), Mei, Liu & Yue (1999), Faltinsen (2002) and Korobkin (2004), a combination of at least two of the following modifications to the leading-order theory is employed:

- (i) retaining a nonlinear term in one or more of the boundary conditions or in the Bernoulli condition for the pressure on the impactor;
- (ii) linearizing the boundary conditions onto the line drawn through the jet roots, rather than onto the location of the undisturbed free surface;
- (iii) applying Wagner’s theory to the free surface, but not to the body profile, for a body of finite deadrise angle on which the full kinematic boundary condition is retained;
- (iv) evaluating the upward force by integrating the pressure on the body over the segment where it is positive or over the segment below the initial waterline.

Even though these so-called generalized Wagner theories are based on *ad hoc* approximations, the resulting predictions for the upward force are in surprisingly good agreement with numerical solutions of the similarity formulation for wedge entry by Dobrovolskaya (1969), with numerical solutions of the full problem or with experimental data. With regard to obtaining justification for these approximations Korobkin (2004) notes the following. “One may expect that the formal asymptotic analysis of the entry problem by means of the method of matched asymptotic expansions including higher-order terms and matching properly the outer expansion (in the main flow region) with the inner expansion (in the jet region) would be more promising. Up to now even the second-order asymptotic solution of the

† Faltinsen (1990), Howison *et al.* (1991) and Korobkin (1996), for example, discuss how this statement must be made with the caveat that in practice Wagner’s theory is not applicable at very small deadrise angles (of less than approximately 5°), the effects of air cushioning becoming increasingly important as the zero-deadrise-angle limit is approached.

two-dimensional impact problem has not been obtained.” This statement provides the mathematical motivation for this paper.

The second-order analysis presented in this paper is closest to the analyses of Cointe & Armand (1987), Fontaine & Cointe (1998), Oliver (2002) and Korobkin (2006), with the following differences. Cointe & Armand (1987) and Fontaine & Cointe (1998), who considered a circular cylinder and wedge, respectively, did not solve explicitly the relevant second-order outer potential problem or account for the second-order correction to the locations of the jet root regions. Although the latter was accounted for by Oliver (2002), the analysis was not taken to second order. Korobkin (2006) presented a second-order analysis for the closely related problem of the uniform-normal impact of a liquid parabola onto a rigid flat plate; his analysis involved a non-standard transformation of the dependent variables, which, as will become apparent, is only applicable to this special case because the jet roots lie at leading order on the plate on which the boundary conditions in the outer region are linearized and imposed.

The outline of the paper is as follows. In §2 the problem is formulated and the formal asymptotic structure in the small-deadrise-angle regime is described. In §3 the well-known leading-order outer analysis is reviewed and extended to obtain the higher-order terms in the expansions of the leading-order variables at their points of non-uniformity. These terms and a non-local transformation of the leading-order outer solution are required for the second-order outer analysis, which is described in §4. In §5 the second-order correction to the upward force on the impactor is described. The details of the solutions in the inner regions, matching and force calculation are given in the Appendices. In §6 three applications of the second-order theory are described and comparisons made with numerical and experimental data. A summary of the main results and of their theoretical and practical implications is given in §7.

2. Problem statement and asymptotic structure

The majority of this paper is devoted to the two-dimensional normal impact of a rigid symmetric body of small deadrise angle on a half-space of ideal and incompressible liquid. As in the theory of Wagner (1932), viscosity, gravity, compressibility, surface tension and air cushioning effects are neglected, and the impactor is assumed to be moving with constant downward velocity V . Cartesian coordinates (x^\dagger, y^\dagger) are introduced, with origin at the point of impact at time $t^\dagger = 0$. Initially the liquid is stationary and lies in the lower half-plane $y^\dagger < 0$. The location of the impactor is denoted by $y^\dagger = Lf(\epsilon x^\dagger/L) - Vt^\dagger$, where L is a typical penetration distance and the body profile f is an even function of x^\dagger such that $f(0) = 0$, $f'(\epsilon x^\dagger/L) > 0$ for $\epsilon x^\dagger/L > 0$, where f' denotes the derivative of f with respect to its argument, and $f(\epsilon x^\dagger/L) = O(1)$ for $|\epsilon x^\dagger| = O(L)$ in the small-deadrise-angle regime in which $\epsilon \ll 1$. The velocity potential, multi-valued free surface, pressure and upward force on the impactor (per distance L in the direction perpendicular to the (x^\dagger, y^\dagger) -plane) are denoted by $\phi^\dagger(x^\dagger, y^\dagger, t^\dagger)$, $y^\dagger = h^\dagger(x^\dagger, t^\dagger)$, $p^\dagger(x^\dagger, y^\dagger, t^\dagger)$ and $F^\dagger(t^\dagger)$, respectively. The governing equations are non-dimensionalized on the penetration depth by setting

$$x^\dagger = Lx^*, \quad y^\dagger = Ly^*, \quad t^\dagger = \frac{Lt}{V}, \quad \phi^\dagger = LV\phi^*, \quad h^\dagger = Lh^*, \quad p^\dagger = \rho V^2 p^*, \quad F^\dagger = \rho V^2 L F^*,$$

where ρ is the constant liquid density. The dimensionless model problem is

$$\nabla^{*2} \phi^* = 0, \tag{2.1}$$

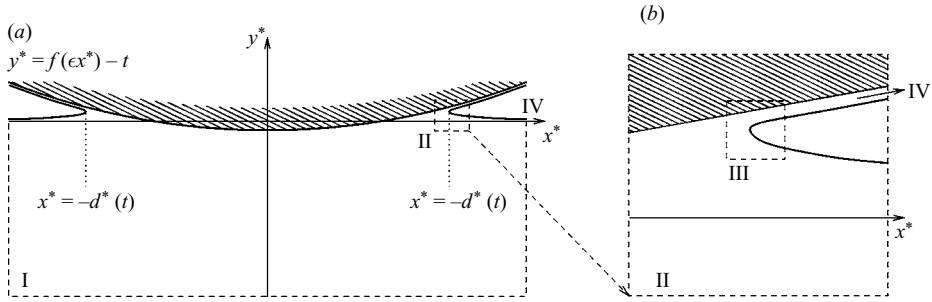


FIGURE 1. Asymptotic structure in the small-deadrise-angle regime $\epsilon \ll 1$ (a) showing the inner regions near the right-hand turnover point (b): outer region (I) of size $O(1/\epsilon)$; (artificial) intermediate region (II) of size $O(1)$; inner jet-root region (III) on the body of size $O(\epsilon)$; jet region (IV) on the body of horizontal extent $O(1/\epsilon)$ and of thickness $O(\epsilon)$.

in the fluid region of figure 1, with the kinematic condition on the body that

$$\text{on } y^* = f(\epsilon x^*) - t: \quad \frac{\partial \phi^*}{\partial y^*} = -1 + \epsilon f'(\epsilon x^*) \frac{\partial \phi^*}{\partial x^*}, \quad (2.2)$$

and the kinematic and Bernoulli conditions on the free surfaces that

$$\text{on } y^* = h^*(x^*, t): \quad \frac{\partial \phi^*}{\partial n} = v_n^*, \quad p^* = 0, \quad (2.3a, b)$$

where $\partial/\partial n$ denotes the outward normal derivative to, and v_n^* the normal velocity of, the relevant free surface and the pressure is given by the Bernoulli equation

$$p^* = -\frac{\partial \phi^*}{\partial t} - \frac{1}{2} |\nabla^* \phi^*|^2. \quad (2.4)$$

The ‘turnover points’ are defined in this paper to be the points of upward tangency of the free surface, with x^* -coordinates denoted by $\pm d^*(t)$, as illustrated in figure 1. As in all previous applications of Wagner’s theory, the initial and far-field conditions are taken to be (writing $r^{*2} = x^{*2} + y^{*2}$)

$$\phi^*(x^*, y^*, 0) = 0, \quad h^*(x^*, 0) = 0, \quad d^*(0) = 0; \quad (2.5a-c)$$

$$\text{as } y^* \rightarrow -\infty: \quad \phi^* = O(1/r^*); \quad \text{as } |x^*| \rightarrow \infty: \quad h^* \rightarrow 0. \quad (2.6a, b)$$

As described by Korobkin & Pukhnachov (1988), Faltinsen (1990) and Korobkin (1996), for example, the effects of compressibility and surface tension are restricted to an initial time interval, T say, that is typically much smaller than L/V for a wide class of water impact problems in which the effects of viscosity become important on time scales much larger than L/V or in very thin boundary layers on the impactor on the time scale L/V . The good agreement with experiment of numerous predictions of the leading-order theory provide strong evidence that the small-time limit of the Wagner model (that is applicable on the time scale L/V) is consistent with the long-time limit of the full model (that is applicable on the time scale T and incorporates the effects of compressibility, viscosity and surface tension), and hence for the validity of the initial conditions (2.5). The far-field condition (2.6a) is a necessary condition for bounded spatially integrated kinetic energy, while (2.6b) corresponds to the assumption that the free surface asymptotes to its undisturbed elevation far from the point of impact.

The primary aim of this paper is to find the second-order correction to the upward force on the impactor. Denoting by Γ the *a priori* unknown wetted region lying in

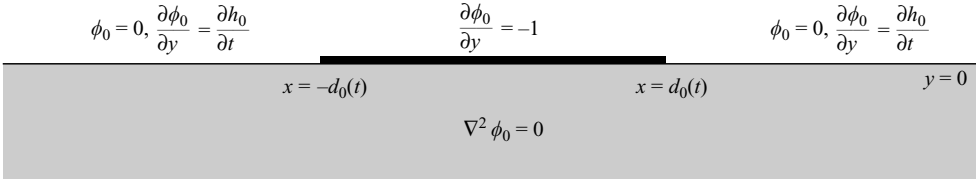


FIGURE 2. Mixed-boundary-value problem for the potential ϕ_0 in outer region I; the initial conditions are $\phi_0(x, y, 0) = 0$, $h_0(x, 0) = 0$ and $d_0(0) = 0$; the far-field conditions are $\phi_0 = O(1/r)$ as $y \rightarrow -\infty$, where $r^2 = x^2 + y^2$, and $h_0 \rightarrow 0$ as $|x| \rightarrow \infty$; the matching conditions at the free points, $z = \pm d_0(t)$, are described in the text.

$|x^*| < c^*(t)$ say, by θ^* the angle between the upward pointing normal to the impactor and the positive y^* -axis and by s^* the tangential coordinate around the impactor in the positive x^* -direction (with origin at $x^* = 0$, say), the upward force is given by

$$F^*(t) = \int_{\Gamma} p^*(x^*, f(\epsilon x^*) - t, t) \cos \theta^* ds^* = 2 \int_0^{c^*(t)} p^*(x^*, f(\epsilon x^*) - t, t) dx^*, \quad (2.7)$$

where in the second equality the symmetry of the flow about the y^* -axis and the expression $dx^*/ds^* = \cos \theta^*$ have been used.

It is shown in detail by, for example, Cointe & Armand (1987), Cointe (1989), Greenhow (1987), Howison *et al.* (1991), Korobkin (1996) and Oliver (2002), that in the small-deadrise-angle regime the configuration just after impact is as illustrated in figure 1, wherein two thin jets are being ejected along the body from two small jet-root regions. In this paper Van Dyke’s matching rule is used to match the solution in region I with the one in region III by introducing an intermediate region II between them of size of the order of the penetration depth (see figure 1). This methodology is based on the one used by Oliver (2002), Howison, Ockendon & Oliver (2002), Howison, Ockendon & Oliver (2004) and Howison *et al.* (2005). The symmetry of the flow about the y^* -axis is used throughout to simplify the analysis. It is convenient to work with the complex potential $w^*(z^*, t) = \phi^* + i\psi^*$, where $z^* = x^* + iy^*$ and $\psi^*(x^*, y^*, t)$ is the stream function; the latter is taken to tend to zero at infinity, without loss of generality, so that ψ^* is equal to zero on the y^* -axis.

3. Leading-order Wagner theory

The size of the outer region away from the jet roots is determined by the distance between them, which is of $O(1/\epsilon)$ when the penetration depth t is of $O(1)$. The outer scalings are therefore given by

$$z^* = \frac{z}{\epsilon}, \quad w^* = \frac{w}{\epsilon}, \quad h^* = h, \quad d^* = \frac{d}{\epsilon}. \quad (3.1)$$

The boundary conditions that follow from (2.2)–(2.3) are linearized and imposed on $y = 0$, while w , h and d are expanded as the asymptotic series

$$w = w_0 + \epsilon w_1 + o(\epsilon), \quad h = h_0 + \epsilon h_1 + o(\epsilon), \quad d = d_0 + \epsilon d_1 + \epsilon^2 d_2 + o(\epsilon^2), \quad (3.2a-c)$$

with the leading- and second-order outer potential and stream function being defined by $w_j = \phi_j + i\psi_j$ ($j = 1, 2$). At leading order the resulting mixed boundary value problem for ϕ_0 is shown in figure 2; the initial and far-field conditions in the caption follow directly from (2.5)–(2.6). It is shown in Appendix B that matching with the leading-order solution in the inner-jet-root region in Appendix A leads to the following

matching conditions at the right-hand free point:

$$\text{as } z \rightarrow d_0(t): \quad w_0(z, t) \sim id_0(t) - 4i\dot{d}_0(t)(H_J(t)(z - d_0(t))/\pi)^{1/2}, \quad (3.3)$$

$$\text{at } x = d_0(t): \quad h_0(x, t) = f(d_0(t)) - t, \quad (3.4)$$

where the overdot denotes the time derivative and $H_J(t)$ is the leading-order thickness of the splash jet ejected from each of the jet roots, as illustrated in figure 8. Similar conditions at the left-hand free point or the symmetry of the flow about the y -axis close the problem. At the free points the square-root singularities in the leading-order outer complex potential dictated by (3.3) result in inverse-square-root singularities in the leading-order outer pressure (see Appendix C), reflecting the leading-order fluid response to the high pressure in the inner jet-root regions associated with the reversal of flow direction in each of them (see Appendix A). As alluded to in § 1, the so-called Wagner conditions (3.4) reflect the fact that at leading order the jet-root regions, which are a factor of the deadrise angle squared smaller than the outer one, lie on the body, so that the outer free surface must ‘rise up’ to meet the impactor at the free points.

The leading-order fluid response is as if the body were an expanding flat plate in the contact set between the free points, moving instantaneously with unit downward velocity, with the solution being the usual one given by

$$w_0(z, t) = i(z - (z^2 - d_0(t)^2)^{1/2}); \quad (3.5)$$

the term containing the square root is defined on the plane cut along $(-d_0(t), d_0(t))$ on the x -axis, with $(x^2 - d_0(t)^2)^{1/2}$ being real and positive (negative) for $x > d_0(t)$ ($x < -d_0(t)$). The kinematic boundary condition on the non-contact set in figure 2 implies that the leading-order elevation of the free surface is given by

$$h_0(x, t) = -t + \int_0^t \frac{|x|}{(x^2 - d_0(\tau)^2)^{1/2}} d\tau, \quad (3.6)$$

the integral being real and bounded for $|x| \geq d_0(t)$ (in accordance with (3.4); see (3.8)) if and only if the free points are advancing (i.e. $\dot{d}_0(t) > 0$), which will be verified *a posteriori*. The local expansions of (3.5)–(3.6) at the right-hand free point are given by

$$\text{as } z \rightarrow d_0(t): \quad w_0 \sim id_0(t) - i(2d_0(t)(z - d_0(t)))^{1/2} + i(z - d_0(t)), \quad (3.7)$$

$$\text{as } x \downarrow d_0(t): \quad h_0 \sim f(d_0(t)) - t - \frac{(2d_0(t)(x - d_0(t)))^{1/2}}{\dot{d}_0(t)} + h_0^\dagger(t)(x - d_0(t)), \quad (3.8)$$

where the last term in each of them is required for the matching in Appendix B and

$$h_0^\dagger(t) = \int_0^t \frac{1}{(d_0(t)^2 - d_0(\tau)^2)^{1/2}} \frac{\partial}{\partial \tau} \left(\frac{d_0(\tau)}{\dot{d}_0(\tau)} \right) d\tau, \quad (3.9)$$

so that (3.5)–(3.6) satisfy the matching conditions (3.3)–(3.4) provided

$$H_J(t) = \frac{\pi d_0(t)}{8\dot{d}_0(t)^2}, \quad \int_0^t \frac{d_0(\tau)d\tau}{(d_0(t)^2 - d_0(\tau)^2)^{1/2}} = f(d_0(t)). \quad (3.10a, b)$$

Expression (3.10a) determines in terms of $d_0(t)$ the thickness of the jet ejected from each of the jet roots, while (3.10b) is an Abel integral equation for $d_0(t)$, which as described by Howison *et al.* (1991), for example, may be inverted to give the algebraic

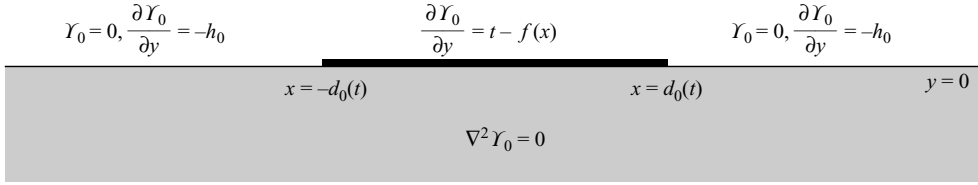


FIGURE 3. Mixed-boundary-value problem for the displacement potential γ_0 in outer region I. In addition, the initial conditions are $\gamma_0(x, y, 0) = 0$ and $d_0(0) = 0$; the far-field conditions are $\gamma_0 = O(1/r)$ as $y \rightarrow -\infty$; the first partial derivatives of γ_0 are continuous at the free points.

equation

$$\int_{-d_0(t)}^{d_0(t)} \frac{(f(\xi) - t) d\xi}{(d_0(t)^2 - \xi^2)^{1/2}} = 0. \tag{3.11}$$

Making the change of variables $\xi = d_0(t) \sin \theta$ and differentiating with respect to t gives

$$\dot{d}_0(t) \int_0^{\pi/2} f'(d_0(t) \sin \theta) \sin \theta d\theta = \frac{\pi}{2}, \tag{3.12}$$

confirming that the free points are advancing, since, by assumption, $f(0) = 0$ and $f'(x) > 0$ for $x > 0$; (3.12) is also used in §4 and in Appendix B. This completes the solution of the leading-order outer problem. For the purposes of this paper three points are noted.

First, writing the kinematic condition on the the free surface in terms of leading-order outer stream function, ψ_0 , which satisfies $\psi_0(d_0(t), 0, t) = d_0(t)$ and $\psi_0(\infty, 0, t) = 0$, implies that the rate of change of the cross-sectional area of the right-hand outer ‘splash-up’ region is given by

$$\frac{\partial}{\partial t} \left(\int_{d_0(t)}^{\infty} h_0(x, t) dx \right) = d_0(t) - \dot{d}_0(t) h_0(d_0(t), t). \tag{3.13}$$

Wilson (1989) noted that this expression may be written in the form

$$\frac{\partial}{\partial t} \left(\int_0^{d_0(t)} (f(x) - t) dx + \int_{d_0(t)}^{\infty} h_0(x, t) dx \right) = -\dot{d}_0(t)(h_0(d_0(t), t) - f(d_0(t)) + t),$$

implying that the Wagner condition (3.4) is a necessary and sufficient condition for leading-order global conservation of mass, i.e. at leading order the outer-splash-up regions are made up of liquid displaced by the impact, with the total cross-sectional area of the splash jets being a factor of $O(\epsilon)$ smaller.

Secondly, there exists a Baiocchi transformation that leads to a useful formulation of the leading-order problem in terms of the displacement potential, which is defined by

$$\gamma_0 = - \int_0^t \phi_0(x, y, \tau) d\tau. \tag{3.14}$$

This function was introduced in the context of the water entry problem by Korobkin (1982) and will feature in the second-order outer analysis in §4. The mixed-boundary-value problem in figure 2 implies the one for the displacement potential in figure 3 in which the condition on the contact set follows from the Wagner condition (3.4).

Howison *et al.* (2004) describe how the relevant (least-singular) solution

$$\frac{\partial \mathcal{Y}_0}{\partial x} - i \frac{\partial \mathcal{Y}_0}{\partial y} = \frac{i(z^2 - d_0(t)^2)^{1/2}}{\pi} \int_{-d_0(t)}^{d_0(t)} \frac{(t - f(\xi))}{(d_0(t)^2 - \xi^2)^{1/2} (\xi - z)} d\xi \quad (3.15)$$

has the far-field expansion

$$\frac{\partial \mathcal{Y}_0}{\partial x} - i \frac{\partial \mathcal{Y}_0}{\partial y} = \frac{i}{\pi} \int_{-d_0(t)}^{d_0(t)} \frac{(f(\xi) - t) d\xi}{(d_0(t)^2 - \xi^2)^{1/2}} + O(1/z^2),$$

as $y \rightarrow -\infty$, so that the far-field condition for \mathcal{Y}_0 in the caption to figure 3 can only be satisfied if (3.11) pertains, i.e. (3.11) is both the consistency condition for existence of the solution to the corresponding Riemann boundary-value problem (that is bounded at the free points and zero at infinity; see, for example, Gakhov 1966) and the inverse of (3.10b).

Thirdly, assuming that the splash jets do not separate from the body, the relevant scalings for the tangential coordinate, tangential velocity and jet thickness in the right-hand one are given by

$$s^* = \frac{s}{\epsilon}, \quad \frac{\partial \phi^*}{\partial s^*} = \frac{u}{\epsilon}, \quad f(x) - t - h = \epsilon \eta(s, t). \quad (3.16)$$

As described by Wilson (1989), for example, at leading order the slender and rapidly moving splash jet is governed by the zero-gravity shallow-water equations

$$\text{for } d_0(t) < s < c_0(t): \quad \frac{\partial u_0}{\partial t} + u_0 \frac{\partial u_0}{\partial s} = 0, \quad \frac{\partial \eta_0}{\partial t} + \frac{\partial}{\partial s} (\eta_0 u_0) = 0, \quad (3.17)$$

where $c_0(t)$ denotes the leading-order location of the end of the jet (so that $\eta_0(c_0(t), t) = 0$), the leading-order tangential velocity u_0 is independent of the coordinate normal to the impactor and η_0 denotes the leading-order thickness of the jet. Moreover, matching with the inner jet-root region gives the boundary data

$$\text{on } s = d_0(t): \quad u_0 = 2\dot{d}_0(t), \quad \eta_0 = H_J(t), \quad (3.18)$$

so that at leading order the rate of change of the cross-sectional area of the right-hand splash jet is given by (cf. (4.27))

$$\frac{\partial}{\partial t} \left(\int_{d_0(t)}^{c_0(t)} \eta_0(s, t) ds \right) = \dot{d}_0(t) H_J(t) \quad (3.19)$$

relative to the original dimensionless coordinates (in which the cross-sectional area of the liquid displaced by the impact is of $O(1/\epsilon)$). Howison *et al.* (1991, 2004) show that if the impactor is blunt, so that $f'(x)$ is continuous at the point of impact, the leading-order theory leads to the intriguing prediction that the splash jets extend to infinity immediately after impact, i.e. $c_0(0^+) = \infty$; in contrast, if $f'(x)$ is discontinuous at $x = 0$, such as for the wedge $f(x) = |x|$, then the extent of each of the splash jets is finite.

4. Second-order Wagner theory

Proceeding to second order in the analysis described in §3 leads to the mixed-boundary-value problem for ϕ_1 depicted in figure 4, with the boundary conditions on the x -axis being derived by linearizing and imposing each of their full versions on $y = 0$, substituting the asymptotic expansions (3.2) and rearranging them as follows.

$$\begin{array}{ccc}
 \frac{\partial \phi_1}{\partial y} = \frac{\partial h_1}{\partial t} & & \frac{\partial \phi_1}{\partial y} = \frac{\partial h_1}{\partial t} \\
 \phi_1 = -h_0 \frac{\partial h_0}{\partial t} - h_0 + G(x, t) & \frac{\partial \phi_1}{\partial y} = \frac{\partial}{\partial x} (f(x) - t) \frac{\partial \phi_0}{\partial x} & \phi_1 = -h_0 \frac{\partial h_0}{\partial t} - h_0 + G(x, t) \\
 \hline
 x = -d_0(t) & & x = d_0(t) \qquad y = 0 \\
 \hline
 \nabla^2 \phi_1 = 0
 \end{array}$$

FIGURE 4. Mixed-boundary-value problem for the potential ϕ_1 in outer region I; the function $G(x, t)$ is given by (4.3); the initial conditions are $\phi_1(x, y, 0) = 0$ and $h_1(x, 0) = 0$; the far-field conditions are $\phi_1 = O(1/r)$ as $y \rightarrow -\infty$ and $h_1 \rightarrow 0$ as $|x| \rightarrow \infty$; the matching conditions at $z = \pm d_0(t)$ are described in the text.

The second-order kinematic boundary condition on the body is given by

$$\text{on } y = 0^-, |x| < d_0(t): \quad \frac{\partial \phi_1}{\partial y} = -(f(x) - t) \frac{\partial^2 \phi_0}{\partial y^2} + f'(x) \frac{\partial \phi_0}{\partial x} = \frac{\partial}{\partial x} \left((f(x) - t) \frac{\partial \phi_0}{\partial x} \right),$$

where in the final equality Laplace's equation for ϕ_0 has been used. It will be convenient to write this condition in terms of the second-order outer stream function, ψ_1 , which is equal to zero at the origin, since ψ_1 tends to zero in the far field and the flow is symmetric about the y -axis. Substituting $\partial \phi_1 / \partial y = -\partial \psi_1 / \partial x$ and integrating along the x -axis gives

$$\text{on } y = 0^-, |x| < d_0(t): \quad \psi_1 = (t - f(x)) \frac{\partial \phi_0}{\partial x}; \quad (4.1)$$

by (3.5), the right-hand side of (4.1) has an inverse-square-root singularity at the free points.

The second-order Bernoulli condition on the free surface is given by

$$\text{on } y = 0^-, |x| > d_0(t): \quad \frac{\partial \phi_1}{\partial t} = -h_0 \frac{\partial^2 \phi_0}{\partial y \partial t} - \frac{1}{2} |\nabla \phi_0|^2 = -h_0 \frac{\partial^2 h_0}{\partial t^2} - \frac{1}{2} \left(\frac{\partial h_0}{\partial t} \right)^2,$$

where in the final equality the leading-order kinematic boundary condition on the free surface in figure 2 has been used. Integrating by parts and applying the initial conditions that $\phi_1(x, y, 0) = 0$ and $h_0(x, 0) = 0$ gives

$$\text{on } y = 0, |x| > d_0(t): \quad \phi_1 = -h_0(x, t) \frac{\partial h_0}{\partial t}(x, t) + \frac{1}{2} \int_0^t \left(\frac{\partial h_0}{\partial \tau}(x, \tau) \right)^2 d\tau.$$

To identify the types of singularity at $x = \pm d_0(t)$ in the right-hand side of this expression it is convenient to write it in the form

$$\text{on } y = 0^-, |x| > d_0(t): \quad \phi_1 = -h_0(x, t) \frac{\partial h_0}{\partial t}(x, t) - h_0(x, t) + G(x, t), \quad (4.2)$$

where, by (3.6), the final term is given by (for $|x| > d_0(t)$)

$$G(x, t) = \int_0^t \frac{\partial h_0}{\partial \tau}(x, \tau) + \frac{1}{2} \left(\frac{\partial h_0}{\partial \tau}(x, \tau) \right)^2 d\tau = \int_0^t \frac{d_0(\tau)^2}{2(x^2 - d_0(\tau)^2)} d\tau. \quad (4.3)$$

A standard asymptotic analysis shows that the local expansion of $G(x, t)$ at the right-hand free point is given by

$$\text{as } x \downarrow d_0(t): \quad G(x, t) \sim -\frac{d_0(t)}{4\dot{d}_0(t)} \ln(x - d_0(t)) + G(t), \quad (4.4)$$

where

$$G(t) = -\frac{d_0(t)}{4\dot{d}_0(t)} \ln(2d_0(t)) + \frac{1}{4} \int_0^t \ln(d_0(t)^2 - d_0(\tau)^2) \frac{\partial}{\partial \tau} \left(\frac{d_0(\tau)}{\dot{d}_0(\tau)} \right) d\tau, \quad (4.5)$$

with a similar expansion pertaining at the left-hand one. Thus, the potential on the non-contact set has an inverse-square-root and a logarithmic singularity at the free points, these singularities arising from the first and last terms on the right-hand side of (4.2), respectively, as well as a square-root singularity, with contributions from both the first and second terms, but not from the third one.

The second-order kinematic boundary condition on the free surface is given by

$$\text{on } y = 0^-, |x| > d_0(t): \quad \frac{\partial \phi_1}{\partial y} = -\frac{\partial^2 \phi_0}{\partial y^2} h_0 + \frac{\partial h_1}{\partial t} + \frac{\partial h_0}{\partial x} \frac{\partial \phi_0}{\partial x} = \frac{\partial h_1}{\partial t}, \quad (4.6)$$

where in the final equality Laplace's equation and the Bernoulli condition for ϕ_0 in figure 2 have been used.

As in the leading-order problem, the far-field conditions in the caption to figure 4 follow directly from (2.5)–(2.6). It is shown in Appendix B that the matching conditions at $z = d_0(t)$ that (together with the symmetry of the flow about the y -axis) close the second-order outer problem are given by

$$\text{as } z \rightarrow d_0(t): \quad w_1(z, t) \sim \frac{id_0(t)(d_1(t) + i(f(d_0(t)) - t))}{(2d_0(t)(z - d_0(t)))^{1/2}}, \quad (4.7)$$

$$\text{as } x \downarrow d_0(t): \quad h_1(x, t) \sim \frac{d_0(t)d_1(t)}{\dot{d}_0(t)(2d_0(t)(x - d_0(t)))^{1/2}} - H_J(t), \quad (4.8)$$

in terms of $d_1(t)$, the second-order correction to the location of the right-hand turnover point, and of $H_J(t)$, the leading-order thickness of the jet that is ejected from each of the jet roots. The inverse-square-root singularity on the right-hand side of (4.7) reflects the response of the second-order outer flow to the second-order correction to the location of right-hand jet root, which is of size of $O(\epsilon^2)$ relative to the outer coordinates and lies on the body at $z = d_0(t) + \epsilon(d_1(t) + i(f(d_0(t)) - t) + o(\epsilon))$, rather than at the free point $z = d_0(t)$; the horizontal component of this small translation, $\epsilon d_1(t)$, drives the inverse-square-root singularity on the right-hand side of (4.8).

The solution may be constructed in three steps by writing $w_1 = w_{1,1} + w_{1,2} + w_{1,3}$, where for $j = 1, 2, 3$, $w_{1,j} = \phi_{1,j} + i\psi_{1,j}$ are as follows. First, the boundary conditions for ϕ_0 and γ_0 in figures 2 and 3 imply that the complex potential

$$w_{1,1} = -\left(\frac{\partial \gamma_0}{\partial x} - i \frac{\partial \gamma_0}{\partial y} \right) \left(\frac{\partial \phi_0}{\partial x} - i \frac{\partial \phi_0}{\partial y} - i \right) \quad (4.9)$$

satisfies the mixed-boundary conditions

$$\text{on } y = 0^-, |x| < d_0(t): \quad \psi_{1,1} = (t - f(x)) \frac{\partial \phi_0}{\partial x}, \quad (4.10)$$

$$\text{on } y = 0^-, |x| > d_0(t): \quad \phi_{1,1} = -h_0 \left(1 + \frac{\partial h_0}{\partial t} \right). \quad (4.11)$$

Since $\phi_{1,1}$ decays as the inverse square of distance in the far field, it is the least-singular solution to the mixed-boundary-value problem in figure 4 with $G(x, t)$ replaced by zero in the Bernoulli condition. Moreover, since $w_{1,1}$ has an inverse-square-root singularity at the right-hand free point given by (4.7) with $d_1(t)$ replaced by zero, $w_{1,1}$ is the complex potential of second-order outer flow driven by the small vertical

displacements of the jet roots above the undisturbed waterline. Secondly, to account for $G(x, t)$ being non-zero and given by (4.3), it is necessary to solve for the complex potential $w_{1,2}$ that is zero at infinity, least singular at the free points and satisfies the mixed boundary conditions

$$\text{on } y = 0^-, |x| < d_0(t): \quad \psi_{1,2} = 0, \quad (4.12)$$

$$\text{on } y = 0^-, |x| > d_0(t): \quad \phi_{1,1} = G(x, t). \quad (4.13)$$

A standard application of the theory of Riemann mixed-boundary-value problems implies that

$$w_{1,2} = \frac{i(z^2 - d_0(t)^2)^{1/2}}{\pi} \left(\int_{-\infty}^{-d_0(t)} + \int_{d_0(t)}^{\infty} \right) \frac{G(\xi, t) \operatorname{sgn}(\xi)}{(\xi^2 - d_0(t)^2)^{1/2} (\xi - z)} d\xi \quad (4.14)$$

provided the branch of the multi-valued integral on the right-hand side of this expression is selected to satisfy the boundary conditions (4.12)–(4.13). As described in detail by Gakhov (1966), for example, this is because $G(x, t)$ is Hölder continuous except at the free points, where it has logarithmic singularities given by (4.4), so that the integral is well defined in $y < 0$ and on the contact set, and well defined by its principal value on the non-contact set away from the free points. Moreover, (4.4) implies that $w_{1,2}$ has logarithmic singularities at the free points corresponding to the sinks in the second-order outer potential flow that drive a flux into each of the jet roots; the fate of this liquid is described at the end of this section in the context of the condition for second-order global conservation of mass. That $w_{1,2}$ tends to zero at infinity follows from $G(x, t)$ being an even function of x . In practice the evaluation of (4.14) may be aided by consideration of the analytic continuation of $G(x, t)$ into $y \leq 0$, with the caveat that the branch of the multi-valued function that will inevitably arise in this process is chosen to be consistent with the boundary conditions (4.12)–(4.13); see § 6.1 and § 6.2 for two examples. Thirdly, the eigensolution selected by the matching condition (4.7) is given by

$$w_{1,3} = \frac{iA(t)}{(z^2 - d_0(t)^2)^{1/2}}, \quad (4.15)$$

where $A(t)$ is a real function that will be determined shortly; as described above, the inverse-square-root singularities at the free points in this expression reflect the response of the second-order outer flow to the small horizontal displacements of the jet roots along the body.

By the kinematic condition (4.6) and the fact that $\psi_{1,1}(x, 0, t) = 0$ for $|x| > d_0(t)$, the second-order outer elevation of the free surface is given by $h_1 = h_{1,2} + h_{1,3}$, where (for $|x| > d_0(t)$)

$$h_{1,2}(x, t) = \int_0^t \frac{\partial}{\partial x} \left(\frac{\operatorname{sgn}(x)(x^2 - d_0(\tau)^2)^{1/2}}{\pi} \int_{d_0(\tau)}^{\infty} \frac{2\xi G(\xi, \tau)}{(\xi^2 - d_0(\tau)^2)^{1/2} (x^2 - \xi^2)} d\xi \right) d\tau, \quad (4.16)$$

$$h_{1,3}(x, t) = \int_0^t \frac{A(\tau)|x|}{(x^2 - d_0(\tau)^2)^{3/2}} d\tau. \quad (4.17)$$

A standard asymptotic analysis (see, for example, Gakhov 1966, § 8) results in the following local expansions for w_1 and h_1 at the right-hand free point:

$$\text{as } z \rightarrow d_0(t): \quad w_1 \sim \frac{iA(t) - d_0(t)(f(d_0(t)) - t)}{(2d_0(t)(z - d_0(t)))^{1/2}} - \frac{d_0(t)}{4\dot{d}_0(t)} \ln(z - d_0(t)) + a(t), \quad (4.18)$$

where the principal branch of the logarithm has been taken and

$$a(t) = \frac{d_0(t)}{\dot{d}_0(t)} + G(t) - \frac{i\pi d_0(t)}{4\dot{d}_0(t)}; \quad (4.19)$$

$$\text{as } x \downarrow d_0(t): \quad h_1 \sim \frac{A(t)}{\dot{d}_0(t)(2d_0(t)(x - d_0(t)))^{1/2}} + h_1^\dagger(t), \quad (4.20)$$

where

$$h_1^\dagger(t) = h_{1,2}(d_0(t), t) - \int_0^t \frac{d_0(\tau)}{(d_0(\tau)^2 - d_0(\tau^2))^{1/2}} \frac{\partial}{\partial \tau} \left(\frac{A(\tau)}{d_0(\tau)\dot{d}_0(\tau)} \right) d\tau. \quad (4.21)$$

The local expansion (4.18) is in agreement with (4.7), as is (4.20) with (4.8), provided the matching conditions

$$A(t) = d_0(t)d_1(t), \quad h_1^\dagger(t) = -H_J(t) \quad (4.22a, b)$$

pertain. Since (4.22a) gives $A(t)$ in terms of $d_1(t)$, the second-order-Wagner condition (4.22b) leads to the singular-integral equation

$$\int_0^t \frac{d_0(\tau)}{(d_0(\tau)^2 - d_0(\tau^2))^{1/2}} \frac{\partial}{\partial \tau} \left(\frac{d_1(\tau)}{\dot{d}_0(\tau)} \right) d\tau = H_J(t) + h_{1,2}(d_0(t), t) \quad (4.23)$$

for $d_1(t)$. By (3.10a), (3.12) and (4.16), the right-hand side of (4.23) may be written as a function of $d_0(t)$:

$$H_c(d_0) = \frac{d_0}{2\pi} \left(\int_0^{\pi/2} f'(d_0 \sin \theta) \sin \theta d\theta \right)^2 + h_{1,2}(d_0, \omega(d_0)), \quad (4.24)$$

where $t = \omega(d_0)$ is the inverse of $d_0 = d_0(t)$. Hence, (4.23) may be inverted to give

$$d_1(t) = \frac{2\dot{d}_0(t)}{\pi} \int_0^{\pi/2} H_c(d_0(t) \sin \theta) d\theta. \quad (4.25)$$

This completes the solution of the second-order outer problem. The complexity of the expressions for $\partial\mathcal{Y}_0/\partial x - i\partial\mathcal{Y}_0/\partial y$, $w_{1,2}$, $h_{1,2}$ and H_c has restricted further analytic progress to specific body profiles such as those described in §6.

By (3.10a), the sink at the right-hand free point corresponding to the logarithmic term in (4.18) drives a liquid flux $2\dot{d}_0(t)H_J(t)$ into the right-hand jet root; the inner solution reviewed in Appendix A implies that half of this flux is ejected into the right-hand splash jet in accordance with (3.19), while the other half is ‘swept back’ under the impactor. To check that this is consistent with the condition for second-order global conservation of mass note that the kinematic and far-field conditions in figure 4, together with the local expansions (4.18) and (4.20), imply that the second-order version of (3.13) is given by

$$\frac{\partial}{\partial t} \left(\int_{d_0(t)}^{\infty} h_1(x, t) dx \right) = -2\dot{d}_0(t)H_J(t) - \dot{d}_0(t)h_1(t). \quad (4.26)$$

Hence, the second-order Wagner condition (4.22b) is a necessary and sufficient condition for second-order global conservation of mass, which is given by

$$\int_{d_0(t)}^{\infty} h_1(x, t) dx + \int_0^t \dot{d}_0(\tau)H_J(\tau) d\tau = 0, \quad (4.27)$$

i.e. the decrease in the total cross-sectional area of the outer splash-up regions due to the second-order correction to the elevation of the free surface is equal to the total cross-sectional area of the splash jets.

5. The upward force on the impactor

The asymptotic expansion of (2.7) is found by splitting the range of integration into segments corresponding to each of the regions I, II, III and IV, expanding each of them and summing their contributions. In Appendix C it is shown that the resulting expansion for the upward force on the impactor is given by

$$F^*(t) = \frac{F_0(t)}{\epsilon^2} + \frac{F_1(t)}{\epsilon} + o(\epsilon^{-1}), \quad (5.1)$$

where the leading-order term

$$F_0(t) = \pi d_0(t) \dot{d}_0(t) \quad (5.2)$$

receives the usual contribution from only the leading-order outer pressure, while the second-order term

$$F_1(t) = 2\dot{d}_0(t)G(t) - \frac{d_0(t)}{2} \ln(2d_0(t)) - 2\frac{\partial}{\partial t} \left(\int_0^{d_0(t)} \phi_1(x, 0, t) dx \right) \quad (5.3)$$

in which $G(t)$ is given by (4.5), receives contributions from both the second-order outer pressure and from the leading-order jet-root pressure, but not from the intermediate region (as required) or from the splash jets. At leading order the pressure on the impactor takes its maximum value of $\dot{d}_0(t)^2/2\epsilon^2$ at the relative stagnation points in each of the jet-root regions (see figure 8); to obtain the second-order correction to this prediction it is necessary to solve the second-order jet-root problem, an analysis that is not pursued here.

6. Applications

This section begins with an application of the second-order Wagner theory of §2–§5 to the symmetric impact of a wedge. The predictions for the location of the turnover points and for the upward force are compared with those of the similarity solution derived by Dobrovol'skaya (1969) via the numerical solution by Zhao & Faltinsen (1993). The second-order theory for the symmetric impact of a parabola is then described, and the prediction for the upward force is compared to the experimental data of Campbell & Weynberg (1980) and of Cointe & Armand (1987). Finally, the results of applying the second-order theory to the symmetric impact of a solid parabola onto a liquid one are outlined.

6.1. The symmetric impact of a wedge

For the wedge $f(x) = |x|$ the flow is self-similar, with $d_0(t) = \alpha_0 t$, $d_1(t) = \alpha_1 t$, where α_0 and α_1 are real constants. The expressions (3.6), (3.10a) and (3.11) give

$$\text{for } |x| > \alpha_0 t: \quad h_0(x, t) = -t + \frac{x}{\alpha_0} \sin^{-1} \left(\frac{\alpha_0 t}{x} \right), \quad \alpha_0 = \frac{\pi}{2}, \quad H_J(t) = \frac{t}{4}; \quad (6.1)$$

while (3.5) and (3.14) imply that

$$\frac{\partial \gamma_0}{\partial x} - i \frac{\partial \gamma_0}{\partial y} = - \int_0^t \left(\frac{\partial \phi_0}{\partial x} - i \frac{\partial \phi_0}{\partial y} \right) d\tau = -it + \frac{iz}{\alpha_0} \sin^{-1} \left(\frac{\alpha_0 t}{z} \right), \quad (6.2)$$

with appropriate choice of the branch of $\sin^{-1}(\alpha_0 t/z)$, and hence, by (4.9), that

$$w_{1,1} = \left(t - \frac{z}{\alpha_0} \sin^{-1} \left(\frac{\alpha_0 t}{z} \right) \right) \frac{z}{(z^2 - \alpha_0^2 t^2)^{1/2}}. \quad (6.3)$$

An analytic continuation of

$$G(x, t) = -\frac{x}{4\alpha_0} \ln \left(\frac{x - \alpha_0 t}{x + \alpha_0 t} \right) - \frac{t}{2}, \quad |x| > \alpha_0 t,$$

into $y \leq 0$, whose real (imaginary) part is an even (odd) function of x , is given by $G(z, t)$, with the branch cut of the term containing the logarithm being $(-\alpha_0 t, \alpha_0 t)$ on the x -axis, where

$$G((x - i0), t) = -\frac{x}{4\alpha_0} \left(\ln \left| \frac{x - \alpha_0 t}{x + \alpha_0 t} \right| - \begin{cases} i\pi & (|x| < \alpha_0 t) \\ 0 & (|x| > \alpha_0 t) \end{cases} \right) - \frac{t}{2},$$

so that

$$w_{1,2} = -\frac{z}{4\alpha_0} \ln \left(\frac{z - \alpha_0 t}{z + \alpha_0 t} \right) - \frac{t}{2} - \frac{i\pi}{4\alpha_0} (z - (z^2 - \alpha_0^2 t^2)^{1/2}). \quad (6.4)$$

Since $A(t) = d_0(t)d_1(t) = \alpha_0\alpha_1 t^2$ by (4.22a), the second-order outer complex potential is given by

$$w_1 = \left(t - \frac{z}{\alpha_0 t} \sin^{-1} \left(\frac{\alpha_0 t}{z} \right) \right) \frac{z}{(z^2 - \alpha_0^2 t^2)^{1/2}} - \frac{z}{4\alpha_0} \ln \left(\frac{z - \alpha_0 t}{z + \alpha_0 t} \right) - \frac{t}{2} \\ - \frac{i\pi}{4\alpha_0} (z - (z^2 - \alpha_0^2 t^2)^{1/2}) + \frac{i\alpha_0\alpha_1 t^2}{(z^2 - \alpha_0^2 t^2)^{1/2}}, \quad (6.5)$$

and hence (for $|x| > \alpha_0 t$)

$$h_1(x, t) = -\frac{1}{2}h_0(x, t) + \frac{\alpha_1}{\alpha_0^2} \left(\frac{\alpha_0 t|x|}{(x^2 - \alpha_0^2 t^2)^{1/2}} - x \sin^{-1} \left(\frac{\alpha_0 t}{x} \right) \right), \quad (6.6)$$

giving

$$h_1^\dagger(t) = -\frac{1}{2}(\alpha_0 t - t) - \alpha_1 t. \quad (6.7)$$

It follows from the second-order-Wagner condition (4.22b) that

$$\alpha_1 = -\frac{1}{4}(\pi - 3); \quad (6.8)$$

as required this expression is in agreement with both (4.25) and (4.27), and implies that in terms of the original dimensionless variables the locations of the turnover points, $x^* = \pm d^*(t)$, are given by

$$\frac{d^*(t)}{t} = \frac{\pi}{2\epsilon} - \frac{1}{4}(\pi - 3) + o(1), \quad (6.9)$$

Finally, (5.1)–(5.3) imply that the upward force on the wedge is given by

$$\frac{F^*(t)}{t} = \frac{\pi^3}{4\epsilon^2} - \frac{\pi}{\epsilon} \left(2K - 1 + \frac{3\pi^2}{8} - \frac{3\pi}{4} \right) + o(\epsilon^{-1}). \quad (6.10)$$

where $K \approx 0.916$ is Catalan's constant.

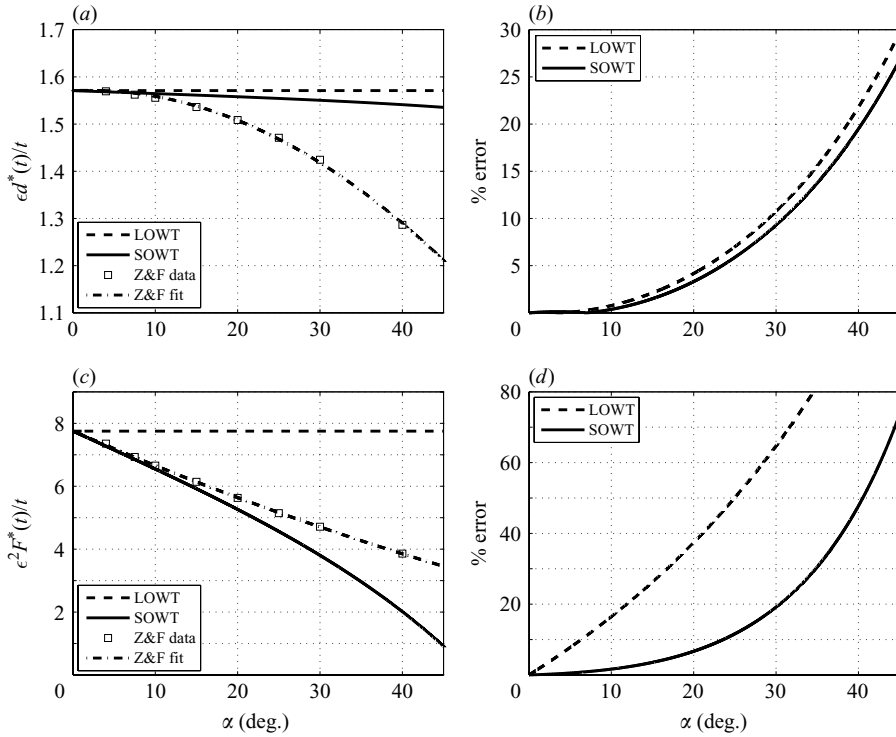


FIGURE 5. Comparison of the predictions of leading-order Wagner theory (LOWT) and of second-order Wagner theory (SOWT) with the numerical data (Z&F data) of Zhao & Faltinsen (1993) for (a) the x^* -coordinate of the right-hand turnover point and (c) the upward force during the uniform normal impact of a wedge of deadrise angle $\alpha = \arctan(\epsilon)$. (b,d) The corresponding percentage errors in the leading- and second-order predictions in (a,c), respectively, based on the best-fit curves (Z&F fit) described in the text. The numerical data are extracted from table 2 of Zhao & Faltinsen (1993) by setting $\epsilon d^*(t)/t = 1 + z_{\max}(t^\dagger)/Vt^\dagger$ and $\epsilon^2 F^*(t)/t = \epsilon^2 F^\dagger(t^\dagger)/\rho V^2 t^\dagger$ in terms of the original dimensional variables and of the y^\dagger -coordinate of the point of maximum pressure, $z_{\max}(t^\dagger)$.

Figures 5(a) and 5(c) contain plots of the predictions for the leading- and second-order x^* -coordinate of the right-hand turnover point and for the upward force, together with the numerical results of Zhao & Faltinsen (1993) for the similarity solution of Dobrovol'skaya (1969). In each of these plots the horizontal ordinate is the deadrise angle, which is given by $\alpha = \arctan \epsilon$, while the vertical ordinate is chosen to magnify the small discrepancies between the predictions and data. These discrepancies are quantified in figures 5(b) and 5(d) by the percentage error of each of them relative to the least-squares best-fit quadratics in α through the numerical data, which have been chosen to intersect at $\alpha = 0$ with the relevant leading-order values predicted by Wagner theory. The second-order prediction for $d^*(t)$ offers a small improvement over the leading-order one, both of them being within 10% of the numerical data for deadrise angles less than about 30° ($\epsilon \approx 0.58$). However, the second-order prediction for the upward force is significantly closer to the numerical data than the leading-order one; figure 5(d) illustrates that the second-order prediction is within 10% of the numerical data for deadrise angles less than about 23.6° ($\epsilon \approx 0.44$), while the leading-order one reaches the same threshold when the deadrise angle is just 6.3°

($\epsilon \approx 0.11$). These observations suggest that the second-order prediction may increase by a factor of about four the domain of applicability of the leading-order one.

It is worth noting that Fraenkel & McLeod (1997) used the all-purpose integral formulation mentioned in §1 to derive expansions for the locations of the high-pressure jet-root regions and for the upward force as the (unknown) contact angle β between the wedge and free surface tends to zero. These expansions imply that, as $\beta \rightarrow 0$,

$$\frac{d^*(t)}{t} = \left(\frac{\pi}{8\beta}\right)^{1/2} - \frac{\pi}{4} + o(1), \quad (6.11)$$

$$\frac{F^*(t)}{t} = 2 \left(\frac{d^*(t)}{t}\right)^3 \cos(\alpha) \left((2\pi\beta)^{1/2} - \frac{8(2K-1)\beta}{\pi} + o(\beta) \right), \quad (6.12)$$

which agree with (6.9)–(6.10) up to second order in ϵ if and only if the contact angle has the expansion

$$\text{as } \epsilon \rightarrow 0: \quad \beta = \frac{\epsilon^2}{2\pi} - \frac{3\epsilon^3}{2\pi^2} + o(\epsilon^3). \quad (6.13)$$

The leading-order term in this expression is in agreement with the leading-order predictions of the theories of Fraenkel & McLeod (1997) and of Wagner (1932), i.e. at leading order the asymptotic theory is in agreement with the small- ϵ limit of the exact one. However, it is not possible to establish whether or not the second-order correction to the contact angle is correct, and hence whether or not the second-order-asymptotic theory is in agreement with the small- ϵ limit of the exact one, without proceeding to second order in at least the jet-root and jet regions, a necessarily complicated analysis that is not pursued here. It is encouraging, however, that the second-order predictions (6.9)–(6.10) are self-consistent in the sense that they are both in agreement with the small- ϵ limit of the exact theory if and only if the single condition (6.13) pertains.

6.2. The symmetric impact of a parabola

For $f(x) = x^2$, expressions (3.6), (3.10b) and (3.11) imply that $d_0 = \pm (2t)^{1/2}$, together with

$$\text{for } |x| > (2t)^{1/2}: \quad h_0(x, t) = -t + x^2 - |x|(x^2 - 2t)^{1/2}, \quad H_J(t) = \pi(t/2)^{3/2}, \quad (6.14)$$

so that (3.5), (3.14) and (4.9) give

$$w_{1,1} = (t - z^2 + z(z^2 - 2t)^{1/2}) \frac{z}{(z^2 - 2t)^{1/2}}. \quad (6.15)$$

An analytic continuation of

$$G(x, t) = -\frac{x^2}{4} \ln \left(1 - \frac{2t}{x^2} \right) - \frac{t}{2}, \quad |x| < (2t)^{1/2}$$

into $y < 0$ is given by $G(z, t)$, with the branch cuts of the term containing the logarithm being $(-2t)^{1/2}, 0$ and $(0, (2t)^{1/2})$ on the x -axis, where

$$G(x - i0, t) = -\frac{x^2}{4} \left(\ln \left| 1 - \frac{2t}{x^2} \right| - \begin{cases} i\pi \operatorname{sgn}(x) & (0 < |x| < (2t)^{1/2}) \\ 0 & (|x| > (2t)^{1/2}) \end{cases} \right) - \frac{t}{2}.$$

Hence, writing $w_{1,2}(z, t) = G(z, t) + \check{w}_1(z, t)$, with $\check{w}_1 = \check{\phi}_1 + \check{\psi}_1$, it remains to solve for the complex potential \check{w}_1 that is least singular at the free points, zero at infinity and

satisfies the mixed boundary conditions

$$\begin{aligned} \text{on } y = 0, \quad 0 < |x| < (2t)^{1/2}: \quad & \check{\psi}_1 = -\frac{\pi x^2}{4} \operatorname{sgn}(x), \\ \text{on } y = 0, \quad x > (2t)^{1/2}: \quad & \check{\phi}_1 = 0. \end{aligned}$$

This mixed-boundary-value problem was solved by Korobkin (2006) in his analysis of the normal impact of a liquid parabola onto a planar substrate, with the solution being given by (for $y < 0$)

$$\check{w}_1 = -\frac{1}{4} \left(z^2 \ln \left(\frac{(2t - z^2)^{1/2} - (2t)^{1/2}}{(2t - z^2)^{1/2} + (2t)^{1/2}} \right) - 2(2t(2t - z^2))^{1/2} \right), \quad (6.16)$$

with appropriate choice of the branch of the logarithm. Thus, the second-order outer complex potential is given by

$$\begin{aligned} w_1 = & \frac{t - z^2}{(z^2 - 2t)^{1/2}} + z^2 - \frac{z^2}{4} \ln \left(1 - \frac{2t}{z^2} \right) - \frac{t}{2} \\ & - \frac{1}{4} \left(z^2 \ln \left(\frac{(2t - z^2)^{1/2} - (2t)^{1/2}}{(2t - z^2)^{1/2} + (2t)^{1/2}} \right) - 2(2t(2t - z^2))^{1/2} \right) + \frac{i(2t)^{1/2} d_1(t)}{(z^2 - 2t)^{1/2}}, \end{aligned} \quad (6.17)$$

and hence (for $|x| > (2t)^{1/2}$)

$$\begin{aligned} h_1(x, t) = & \frac{1}{4} \left((4t - 3x^2)x \sin^{-1} \left(\frac{(2t)^{1/2}}{x} \right) + 3|x|(2t(x^2 - 2t))^{1/2} \right) \\ & + \int_0^t \frac{(2\tau)^{1/2} d_1(\tau)|x|}{(x^2 - 2\tau)^{3/2}} d\tau. \end{aligned} \quad (6.18)$$

Remarkably, $H_c(d_0) = 0$ in (4.25), so that $d_1(t) = 0$; in terms of the original dimensionless variables this gives

$$d^*(t) = \frac{(2t)^{1/2}}{\epsilon} + o(1). \quad (6.19)$$

That the second-order term is identically equal to zero for a parabola is an intriguing result that motivates the analysis in § 6.3 and explains why the leading-order theory predicts accurately the locations of the pressure maxima, as described below.

A straightforward integration using (5.1)–(5.3) implies that the upward force on the parabola is given by

$$F^*(t) = \frac{\pi}{\epsilon^2} - \frac{(\pi + 2)}{\epsilon} (2t)^{1/2} + o(\epsilon^{-1}). \quad (6.20)$$

Campbell & Weynberg (1980) and Cointe & Armand (1987) present experimental data for an impacting circular cylinder, which in terms of the original dimensional variables in § 2 is given by $y^\dagger = R - (R^2 - x^{\dagger 2})^{1/2} - Vt^\dagger$, where R is the radius and V is the impact velocity. Assuming that a typical penetration depth L is much smaller than R and non-dimensionalizing as in § 2 implies that as $\epsilon = (L/2R)^{1/2} \rightarrow 0$, with $\epsilon x^* = O(1)$, the circular cylinder becomes $y^* = (\epsilon x^*)^2 - t + O(\epsilon^2)$. Hence, up to second order the circular cylinder is replaced by the parabola $f(x) = x^2$ in the region of applicability of Wagner's theory (as is implicit in the approximate analysis of Cointe & Armand 1987); as alluded to in § 1, this result applies to the normal impact of an arbitrary smooth body, with R being its radius of curvature at the point of impact.

The best-fit curve through the experimental data for the elevation of the pressure maxima in figure 5 of Campbell & Weynberg (1980) implies that the best-fit curve

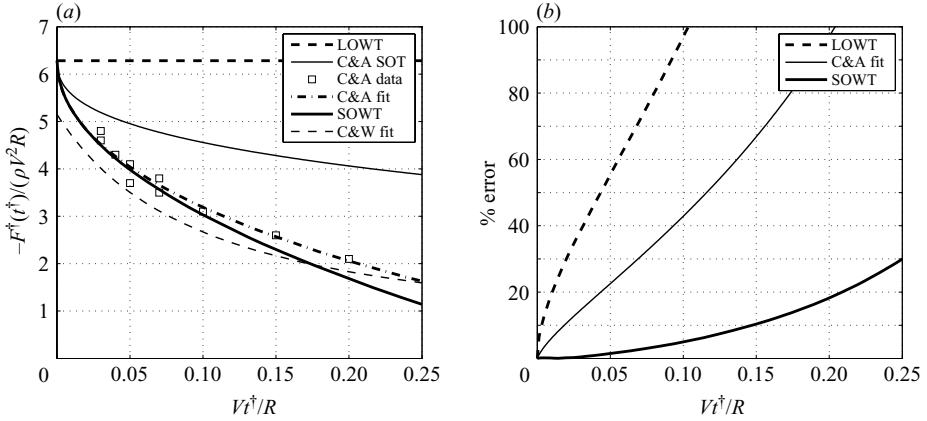


FIGURE 6. (a) Comparison of the predictions of leading-order Wagner theory (LOWT) and of second-order Wagner theory (SOWT) with the experimental data (C&A data) and approximate second-order theory (C&A SOT) of Cointe & Armand (1987) and with the best-fit curve (C&W fit) of Campbell & Weynberg (1980) for the upward force during the impact of a circular cylinder, with downward velocity V and radius R , at penetration depths less than $0.25R$ (for which $\epsilon \approx 0.35$). (b) The percentage error in the leading- and second-order predictions based on the best-fit curve (C&A fit) described in the text.

for the x^\dagger -coordinate of the (right-hand) turnover point is a factor of about 1.05 larger than the one predicted by leading-order Wagner theory for $Vt^\dagger/R < 0.06$, which is consistent with d_1 being equal to zero in this regime. With regard to the upward force, since the dimensional variables are related to the dimensionless ones by $F^\dagger(t^\dagger)/\rho V^2 R = 2\epsilon^2 F^*(t)$ and $Vt^\dagger/R = 2\epsilon^2 t$, ϵ scales out of the dimensional version of the second-order prediction for the upward force (as it must), which is valid for $Vt^\dagger/R \ll 1$ and given by

$$\frac{F^\dagger(t^\dagger)}{\rho V^2 R} = 2\pi - 2(\pi + 2) \left(\frac{Vt^\dagger}{R} \right)^{1/2}.$$

Figure 6(a) contains a plot of the predictions for the leading- and second-order upward force, together with the experimental data and approximate second-order prediction of Cointe & Armand (1987). Figure 6(b) contains the corresponding percentage errors based on the best-fit quadratic in $(Vt^\dagger/R)^{1/2}$ through the experimental data, which has been chosen to intersect at $t^\dagger = 0$ with the leading-order value predicted by Wagner theory. The leading-order theory and the approximate second-order prediction both rapidly over-estimate the upward force, with the percentage errors reaching 10% when Vt^\dagger/R is approximately 0.003 and 0.018, respectively, while the second-order theory is remarkably close to the best-fit curve, with the percentage error reaching 10% when $Vt^\dagger/R \approx 0.15$. These observations suggest that the second-order prediction may increase by two orders of magnitude the domain of applicability of the leading-order one, and by an order of magnitude that of the approximate second-order one. The corresponding best-fit curve through the experimental data of Campbell & Weynberg (1980) is given by

$$\frac{F^\dagger(t^\dagger)}{\rho V^2 R} = \frac{5.15}{1 + 9.5Vt^\dagger/R} + 0.275Vt^\dagger/R$$

for $Vt^\dagger/R < 2$. Although this fit is not necessarily the optimal one for the small times of interest here, it is within 18% of the best-fit curve through the experimental data of Cointe & Armand (1987), and hence, as illustrated in figure 6(a), reasonably close to the prediction of second-order Wagner theory.

6.3. The symmetric impact of a solid parabola onto a liquid one

For the body profile $y^* = \beta_1(\epsilon x^*)^2 - t$ impacting on an initially stationary liquid parabola lying in $y^* < -\beta_2(\epsilon x^*)^2$, where β_1 and β_2 are real constants such that $\beta_1 + \beta_2 > 0$, an analysis paralleling closely the one above gives

$$d^*(t) = \frac{1}{\epsilon} \left(\frac{2t}{\beta_1 + \beta_2} \right)^{1/2} + o(1), \quad (6.21)$$

$$F^*(t) = \frac{\pi}{\epsilon^2(\beta_1 + \beta_2)} - \frac{(\pi + 2)}{\epsilon} \left(\frac{2t}{\beta_1 + \beta_2} \right)^{1/2} + o(\epsilon^{-1}). \quad (6.22)$$

Hence, up to second order the locations of the turnover points and the upward force both depend on the curvature of the body profile, β_1 , and on the curvature of the initial liquid profile, $-\beta_2$, only through the difference between them, $\beta_1 + \beta_2$. This is a manifestation of $d_1(t)$ being equal to zero in this regime, and confirms the conjecture made by Korobkin (2005) that, with an error of $o(d_0)$ as $d_0 \rightarrow 0$, the upward force exerted on a planar substrate by an impacting liquid parabola is equal to the force on a solid parabola of the same shape impacting on a liquid half-space with the same velocity.

7. Discussion

A comprehensive account has been given of second-order Wagner theory for the two-dimensional normal impact of a symmetric body of small deadrise angle on a half-space of liquid. Although the non-uniformities in the outer expansion of the potential at the free points raise serious doubts concerning the accuracy of existing *ad hoc* approximations in which one or more terms in the second-order outer problem are neglected or in which the range of integration in the calculation of the force is truncated, it has been shown that these difficulties can be overcome by a systematic matched-asymptotic analysis. The second-order outer potential problem was solved using the displacement potential of the corresponding leading-order outer one and the theory of Riemann mixed-boundary-value problems, with the relevant eigensolution and closure conditions being determined by matching. One of these closure conditions may be viewed as the second-order version of the well-known Wagner condition and leads to a prediction for the second-order correction to the location of each of the jet-root regions. The expressions describing leading- and second-order global conservations of mass were used to confirm that at leading order the liquid displaced by the impact lies in the splash-up regions, while at second order the decrease in the cross-sectional area of the splash-up regions is equal to the cross-sectional area of the splash jets. The second-order theory led to predictions for the upward force on an impacting wedge and parabola that are consistent with numerical and experimental data, respectively, and extend the range of applicability of the leading-order theory from small to moderate deadrise angles.

In §6.3 the results of applying the second-order theory to the symmetric impact of a solid parabola onto a liquid one were outlined, illustrating that the method of solution of the second-order outer problem in §4 is applicable to water entry

problems with more complicated geometries. For example, the case of oblique impact of an asymmetric body profile at constant velocity can be solved with minor algebraic modifications. These generalizations are superseded, however, by the need for a more comprehensive comparison with experiment, with numerical solutions of the full problem and with the approximate models outlined in §1 of the predictions of the second-order theory, which would be aided by the construction of the second-order jet-root solution and of the resulting composite expansion for the pressure on the body.

With regard to improving further the accuracy of the predictions, it is anticipated that the third-order force on the impactor is a factor of $O(\epsilon^2)$ or $O(\epsilon^2 \ln(1/\epsilon))$ smaller than the leading-order one, since it receives contributions from pressure in the third-order outer, second-order jet-root and leading-order jet regions (see figure 1). The higher-order analysis required to establish the coefficient of the third-order term in the expansion for the force, and whether or not a logarithmic term arises, is therefore necessarily complicated and, for a strictly convex body profile, sensitive to whether or not the splash jets separate, as is often the case in practice. Vanden-Broeck & Keller (1989) showed that even small amounts of surface tension can have a significant effect on the existence and location of a separation point, so the third-order analysis presents in addition some open modelling questions.

In the three-dimensional problem the flow in the jet-root region is quasi-two-dimensional in each of the planes perpendicular to the turnover curve, provided the impactor is sufficiently smooth away from the point of impact. Although some excellent analytical progress has recently been made by Scolan & Korobkin (2001) and Korobkin & Scolan (2006) on the solution of the leading-order outer mixed-boundary-value problem for several classes of three-dimensional body profile, the solution of the corresponding second-order one presents some highly non-trivial challenges for the burgeoning field of higher-order Wagner theory.

The author acknowledges the support of the EPSRC (GR/S93585/01(P)), of the Royal Commission for the Exhibition of 1851 and of Boston University (the latter in the form of a Visiting Scholarship). The author is grateful to Professor L. E. Fraenkel, Dr S. D. Howison, Professor J. R. King, Professor A. A. Korobkin, Dr J. R. Ockendon and the anonymous referees for some useful comments.

Appendix A. Intermediate and inner regions

To match the second-order outer solution with the leading-order one in the right-hand inner jet root using Van Dyke's matching rule it is necessary to introduce an (artificial) intermediate region between them. In this paper the smallest admissible intermediate region, of size of the order of the penetration depth, is employed in order to give an explicit account of the geometric structure that leads to the matching conditions (3.3)–(3.4) and (4.7)–(4.8).

In the right-hand intermediate region the relevant scalings are given by

$$z = d_0 + \epsilon \hat{z}, \quad w = id_0 + \epsilon^{1/2} \hat{w}, \quad h = f(d_0) - t + \epsilon^{1/2} \hat{h},$$

where in terms of $\hat{z} = \hat{x} + i\hat{y}$ the free surface is given by $\hat{y} = \hat{h}(\hat{x}, t)$. The relevant expansions are given by

$$\hat{w}(\hat{z}, t) = \hat{w}_0(\hat{z}, t) + \epsilon^{1/2} \ln(1/\epsilon) b_1(t) + \epsilon^{1/2} \hat{w}_1(\hat{z}, t) + o(\epsilon^{1/2}),$$

$$\hat{h}(\hat{x}, t) = \hat{h}_0(\hat{x}, t) + \epsilon^{1/2} h_1(\hat{x}, t) + o(\epsilon^{1/2}),$$

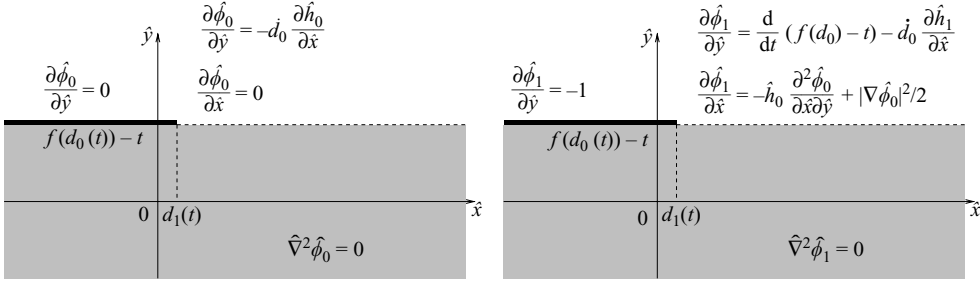


FIGURE 7. The mixed-boundary-value problems for $\hat{\phi}_0$ and $\hat{\phi}_1$ in intermediate region II; see text for the matching conditions in the far field and at $\hat{z} = d_1 + i(f(d_0) - t)$.

where $b_1(t)$ is to be determined by matching. The term id_0 on the right-hand side of the expression for w corresponds to the liquid flux associated with the first term on the right-hand side of (3.13). While the presence of the solely time-dependent term $\epsilon^{1/2} \ln(1/\epsilon)b_1(t)$ in the expansion of \hat{w} may be rather obscure at this point, its lack of significance in the second-order analysis in this paper will become clearer as the various balances are identified (in particular, it has no effect on the flow in the intermediate region up to $O(\epsilon^{3/2} \ln(1/\epsilon))$). At leading order the impactor is horizontal and given by $\hat{y} = f(d_0(t)) - t$, while the inner region is located at $\hat{z} = d_1(t) + i(f(d_0(t)) - t)$, with both $d_0(t)$ and $d_1(t)$ being determined as part of the solutions of the leading- and second-order outer problems. The resulting mixed-boundary-value problems for $\hat{\phi}_0 = \text{Re}(\hat{w}_0)$ and $\hat{\phi}_1 = \text{Re}(\hat{w}_1)$ are shown in figure 7, where the boundary conditions have been linearized and imposed on $\hat{y} = f(d_0) - t$; the motion of the impactor is felt at $O(\epsilon^{1/2})$, but not at leading order. Matching will show that the relevant solutions are the local travelling-wave forms at the right-hand free point of the corresponding leading- and second-order outer solutions, but with no inverse-square-root singularity in the complex potential and translated so that the non-uniformities lie on the body at $\hat{z} = d_1 + i(f(d_0) - t)$, rather than on the undisturbed waterline at $\hat{z} = 0$; thus,

$$\begin{aligned} \hat{w}_0 &= -i(2d_0(\hat{z} - d_1 - i(f(d_0) - t)))^{1/2}, & \hat{h}_0 &= -\frac{(2d_0(\hat{x} - d_1))^{1/2}}{d_0}, \\ \hat{w}_1 &= i\hat{z} - \frac{d_0}{4d_0}(\ln(\hat{z} - d_1 - i(f(d_0) - t)) + i\pi) + b_2, & \hat{h}_1 &= \hat{h}_1^\dagger + f'(d_0)(\hat{x} - d_1), \end{aligned}$$

in which $b_2(t)$ and $\hat{h}_1^\dagger(t)$ to be determined by matching.

The right-hand jet root is of size of the order of the deadrise-angle squared and lies on the body, with the relevant scalings being given by

$$\hat{z} = d_1 + i(f(d_0) - t) + \epsilon Z, \quad \hat{w} = \epsilon^{1/2} W, \quad \hat{h} = \epsilon^{1/2} H,$$

where in terms of $Z = X + iY$ the free surface $Y = H(X, t)$ is multi-valued. It follows that at leading order the turnover point lies at $X = d_2$ and the impactor is horizontal and located at $Y = f'(d_0)d_1$. The relevant expansions are given by

$$W(Z, t) = \ln(1/\epsilon)c_1(t) + W_0(Z, t) + o(1), \quad H(X, t) = H_0(X, t) + o(1),$$

where $c_1(t)$ is to be determined by matching and has no effect on the leading-order flow up to $O(\epsilon^2 \ln(1/\epsilon))$. The kinematic boundary condition on the body is linearized and imposed on $Y = f'(d_0)d_1$, while the boundary conditions on the free surface are linearized and imposed on $Y = H_0(X, t)$. Assuming that the liquid does not separate from the base and writing $\text{Re}(W_0) = d_0 X + \Phi_0$, the familiar leading-order problem

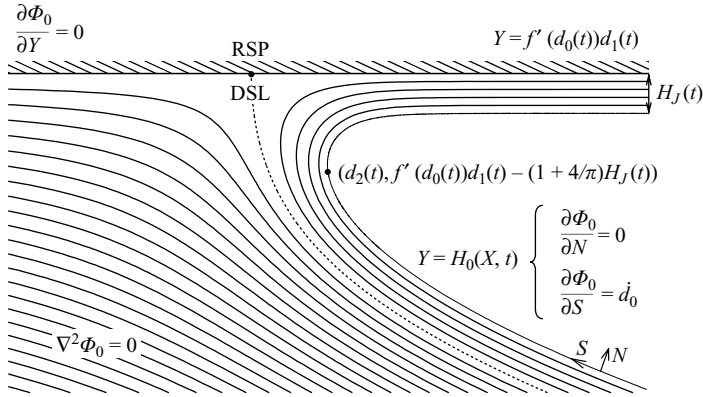


FIGURE 8. The leading-order jet-root problem for $\Phi_0 = -\dot{d}_0 X + \text{Re}(W_0)$ in inner region III showing the streamlines, relative stagnation point (RSP) and dividing streamline (DSL) in the moving frame; S and N denote the tangential and normal coordinates to the (multi-valued) free surface $Y = H_0(X, t)$ in the directions indicated; the far-field matching conditions are $\dot{d}_0 X + \Phi_0 = O(R^{1/2})$ as $Y \rightarrow -\infty$, where $R^2 = X^2 + Y^2$, and $H_0 = O(-X^{1/2})$ as $X \rightarrow \infty$.

for Φ_0 is shown in figure 8; $H_J(t)$ is the thickness of the jet that is ejected along the body with speed $\dot{d}_0(t)$ (relative to the moving frame) and the far-field conditions follow from matching with the intermediate flow, as shown below. As described by Cointe & Armand (1987), Howison *et al.* (1991) and Wagner (1932), for example, the solution to this well-known Helmholtz cavity flow problem for Φ_0 is found by standard conformal mapping methods and implies that the leading-order complex potential in the jet root is given by

$$W_0 = c_2 - \frac{2\dot{d}_0 H_J}{\pi} (2\zeta^{1/2} + \ln \zeta), \quad Z = d_2 + i f'(d_0) d_1 - \frac{H_J}{\pi} (1 + \zeta + 4\zeta^{1/2} + \ln \zeta),$$

where $c_2(t)$ is to be determined by matching; the principal branch of $\ln \zeta$ has been taken in both of these expressions, so that the fluid domain in figure 8 is mapped by the second of them onto the upper half of the ζ -plane. The free surface is given by (for $\zeta = -\xi < 0$)

$$H_0 = -H_J - \frac{4H_J \xi^{1/2}}{\pi}, \quad X = \frac{H_J}{\pi} (\xi - \ln \xi - 1).$$

Half of the liquid flux, $2\dot{d}_0 H_J$, driven into the inner region by the source in the far-field is ejected into the splash jet (via the liquid ‘channelled around’ the free surface in the region between the free surface, the wall and the dividing streamline in the moving frame), while the other half is ‘swept back’ under the impactor (via the liquid in the region below the dividing streamline and the impactor in the moving frame). The leading-order pressure takes its maximum value at the relative stagnation point (see § 5 and Appendix C).

In the far field, as $Y \rightarrow -\infty$,

$$W_0 = -4i\dot{d}_0 \left(\frac{H_J Z}{\pi} \right)^{1/2} - \frac{2\dot{d}_0 H_J}{\pi} (\ln Z + i\pi) + c_3 + O\left(\frac{\ln Z}{Z^{1/2}} \right),$$

where the principal branch of the logarithm has been taken and

$$c_3 = c_2 + \frac{7}{\pi} \dot{d}_0 H_J + \frac{2\dot{d}_0 H_J}{\pi} \ln \frac{H_J}{\pi};$$

likewise, as $X \rightarrow \infty$ the lower free surface is given by

$$H_0 = -4 \left(\frac{H_J X}{\pi} \right)^{1/2} + f'(d_0)d_1 - H_J + O\left(\frac{\ln X}{X^{1/2}}\right).$$

Appendix B. Matching details

The outer (I), intermediate (II) and inner (III) solutions are now matched using Van Dyke's matching rule (in which logarithmic terms in ϵ are treated as being of order unity relative to algebraic ones for the purposes of matching).

Expanding in intermediate variables and to three terms (with respect to powers of $\epsilon^{1/2}$) the three-term outer expansion for the complex potential gives (in the usual notation)

$$\begin{aligned} \text{II}_3\text{I}_3w &= \text{II}_3[w_0(d_0 + \epsilon\hat{z}, t) + \epsilon w_1(d_0 + \epsilon\hat{z}, t)] \\ &= id_0 + \epsilon^{1/2} \left(-i(2d_0\hat{z})^{1/2} + \frac{iA - d_0(f(d_0) - t)}{(2d_0\hat{z})^{1/2}} \right) \\ &\quad + \epsilon \ln(1/\epsilon) \left(\frac{d_0}{4\dot{d}_0} \right) + \epsilon \left(i\hat{z} - \frac{d_0}{4\dot{d}_0} (\ln \hat{z} + i\pi) + a \right). \end{aligned}$$

Expanding in outer variables and to three terms the three-term intermediate expansion for the complex potential gives

$$\begin{aligned} \text{I}_3\text{II}_3w &= id_0 - i(2d_0(z - d_0))^{1/2} + i(z - d_0) + \epsilon \ln(1/\epsilon) \left(b_1 - \frac{d_0}{4\dot{d}_0} \right) \\ &\quad + \epsilon \left(\frac{id_0(d_1 + i(f(d_0) - t))}{(2d_0(z - d_0))^{1/2}} - \frac{d_0}{4\dot{d}_0} (\ln(z - d_0) + i\pi) + b_2 \right). \end{aligned}$$

Applying Van Dyke's matching rule, by writing these expressions in common variables using $z = d_0 + \epsilon\hat{z}$ and equating them, gives

$$A = d_0d_1, \quad b_1 = \frac{d_0}{4\dot{d}_0}, \quad b_2 = a. \quad (\text{B } 1a-c)$$

Similarly, for the free surface

$$\text{II}_3\text{I}_3h = h_0(d_0, t) + \epsilon^{1/2} \left(-\frac{(2d_0\hat{x})^{1/2}}{\dot{d}_0} + \frac{A}{\dot{d}_0(2d_0\hat{x})^{1/2}} \right) + \epsilon(h_0^\dagger\hat{x} + h_1^\dagger),$$

$$\text{I}_3\text{II}_3h = f(d_0) - t - \frac{(2d_0(x - d_0))^{1/2}}{\dot{d}_0} + f'(d_0)(x - d_0) + \epsilon \left(\frac{d_0d_1}{\dot{d}_0(2d_0\hat{x})^{1/2}} + \hat{h}_1^\dagger - f'(d_0)d_1 \right),$$

with $x = d_0 + \epsilon\hat{x}$, giving in addition to (B 1a) the matching conditions

$$h_0(d_0, t) = f(d_0) - t, \quad h_0^\dagger = f'(d_0), \quad h_1^\dagger = \hat{h}_1^\dagger - f'(d_0)d_1. \quad (\text{B } 2a-c)$$

Expanding in inner variables and to three terms the three-term intermediate expansion for the complex potential gives

$$\begin{aligned} \text{III}_3\text{II}_3w &= id_0 + \epsilon \ln(1/\epsilon) \left(b_1 + \frac{d_0}{4\dot{d}_0} \right) \\ &\quad + \epsilon \left(-i(2d_0Z)^{1/2} - \frac{d_0}{4\dot{d}_0} (\ln Z + i\pi) + b_2 + i(d_1 + i(f(d_0) - t)) \right). \end{aligned}$$

Expanding in intermediate variables and to three terms the three-term inner expansion for the complex potential gives

$$\begin{aligned} \text{II}_3\text{III}_3w = id_0 + \epsilon^{1/2} \left(-4id_0 \left(\frac{H_J}{\pi} (\hat{z} - d_1 - i(f(d_0) - t)) \right)^{1/2} \right) \\ + \epsilon \ln(1/\epsilon) \left(c_1 - \frac{2\dot{d}_0 H_J}{\pi} \right) + \epsilon \left(-\frac{2\dot{d}_0 H_J}{\pi} (\ln(\hat{z} - d_1 - i(f(d_0) - t)) + i\pi) + c_3 \right). \end{aligned}$$

Equating these expressions using $\hat{z} = d_1 + i(f(d_0) - t) + \epsilon Z$ gives

$$H_J = \frac{\pi d_0}{8\dot{d}_0^2}, \quad c_1 = b_1 + \frac{d_0}{4\dot{d}_0}, \quad c_3 = b_2 + i(d_1 + i(f(d_0) - t)). \quad (\text{B } 3a-c)$$

Similarly, for the free surface

$$\text{III}_3\text{II}_3h = f(d_0) - t + \epsilon \left(-\frac{(2d_0 X)^{1/2}}{\dot{d}_0} + \hat{h}_1^\dagger \right),$$

$$\text{II}_3\text{III}_3h = f(d_0) - t + \epsilon^{1/2} \left(-4 \left(\frac{H_J}{\pi} (\hat{x} - d_1) \right)^{1/2} \right) + \epsilon (f'(d_0)d_1 - H_J),$$

with $\hat{x} = d_1 + \epsilon X$, giving in addition to (B 3a) the matching condition

$$\hat{h}_1^\dagger = f'(d_0)d_1 - H_J. \quad (\text{B } 4)$$

The matching conditions (B 2a) and (B 3a) confirm that the local expansions (3.3) and (3.4) give the correct local behaviour for w_0 and h_0 at the right-hand free point. The matching condition (B 2b), in which h_0^\dagger is given by (3.9), leads to a singular integral equation for $d_0(t)$, with inverse (3.12), so that (B 2b) is equivalent to the leading-order Wagner condition (B 2a). Combining (B 2c) and (B 4) leads to the second-order Wagner condition that $h_1^\dagger = -H_J$, which together with (B 1a) confirms that (4.7) and (4.8) give the correct local behaviour for w_1 and h_1 at the right-hand free point. Moreover, the functions $b_1(t)$, $b_2(t)$, $c_1(t)$ and $c_2(t)$ in the intermediate and inner solutions above are related to $a(t)$, $d_0(t)$ and $d_1(t)$, all of which are determined as part of the leading- and second-order outer solutions, by

$$b_1 = \frac{d_0}{4\dot{d}_0}, \quad b_2 = a, \quad c_1 = \frac{d_0}{2\dot{d}_0}, \quad c_2 = a + i(d_1 + i(f(d_0) - t)) - \frac{7\dot{d}_0 H_J}{\pi} - \frac{2\dot{d}_0 H_J}{\pi} \ln \frac{H_J}{\pi}. \quad (\text{B } 5)$$

Hence, in particular, it is necessary to proceed to higher order to determine $d_2(t)$, an analysis that is not pursued here.

Appendix C. Expansion of the upward force on the impactor

The asymptotic expansion of (2.7) is found by splitting the range of integration into the contributions from each of the regions by writing $F^*(t) = F_I(t) + F_{II}(t) + F_{III}(t) + F_{IV}(t)$, where

$$F_I(t) = 2 \int_0^{(d-\delta_1)/\epsilon} p^*(x^*, f(\epsilon x^*) - t, t) dx^*, \quad (\text{C } 1)$$

$$F_{II}(t) = 2 \int_{(d-\delta_1)/\epsilon}^{(d-\delta_2)/\epsilon} p^*(x^*, f(\epsilon x^*) - t, t) dx^*, \quad (\text{C } 2)$$

$$F_{III}(t) = 2 \int_{(d-\delta_2)/\epsilon}^{(d+\delta_2)/\epsilon} p^*(x^*, f(\epsilon x^*) - t, t) dx^*, \quad (C3)$$

$$F_{IV}(t) = 2 \int_{(d+\delta_2)/\epsilon}^{c^*} p^*(x^*, f(\epsilon x^*) - t, t) dx^*, \quad (C4)$$

and δ_1 and δ_2 are two small intermediate parameters, with $\epsilon^2 \ll \delta_2 \ll \epsilon \ll \delta_1 \ll 1$.

In the outer region I, $p^* = \epsilon^{-1} p_0 + p_1 + o(1)$, where

$$p_0 = -\frac{\partial \phi_0}{\partial t}, \quad p_1 = -\frac{\partial \phi_1}{\partial t} - \frac{1}{2} \left(\left(\frac{\partial \phi_0}{\partial x} \right)^2 + \left(\frac{\partial \phi_0}{\partial y} \right)^2 \right). \quad (C5)$$

Since (for $|x| < d_0(t)$)

$$p^*(x^*, (f(\epsilon x) - t), t) = \epsilon^{-1} p_0(x, 0, t) + (f(x) - t) \frac{\partial p_0}{\partial y}(x, 0, t) + p_1(x, 0, t) + o(1), \quad (C6)$$

where (for $|x| < d_0(t)$)

$$p_0(x, 0, t) = \frac{d_0 \dot{d}_0}{(d_0^2 - x^2)^{1/2}}, \quad \frac{\partial p_0}{\partial y}(x, 0, t) = 0, \quad p_1(x, 0, t) = -\frac{\partial \phi_1}{\partial t} - \frac{d_0^2}{2(d_0^2 - x^2)}, \quad (C7)$$

it follows that

$$F_I(t) = \frac{2d_0 \dot{d}_0}{\epsilon^2} \sin^{-1} \left(1 - \frac{\delta_1}{d_0} \right) + \frac{d_0}{2\epsilon} \ln \left(\frac{\delta_1}{2d_0 + \delta_1} \right) - \frac{2}{\epsilon} \int_0^{d_0 - \delta_1} \frac{\partial \phi_1}{\partial t} dx + o(\epsilon^{-1}). \quad (C8)$$

In the intermediate region II, $p^* = \epsilon^{-3/2} \hat{p}_0 + \epsilon^{-1} \hat{p}_1 + o(\epsilon^{-1})$, where

$$\hat{p}_0 = d \frac{\partial \hat{\phi}_0}{\partial \hat{x}}, \quad \hat{p}_1 = d \frac{\partial \hat{\phi}_1}{\partial \hat{x}} - \frac{1}{2} \left(\left(\frac{\partial \hat{\phi}_0}{\partial \hat{x}} \right)^2 + \left(\frac{\partial \hat{\phi}_0}{\partial \hat{y}} \right)^2 \right), \quad (C9)$$

Since (for $\hat{x} < d_1(t)$)

$$p(\hat{x}, f(d_0 + \epsilon \hat{x}) - t, t) = \hat{p}_0(\hat{x}, f(d_0) - t, t) + \epsilon^{1/2} \hat{p}_1(\hat{x}, f(d_0) - t, t) + o(\epsilon^{1/2}), \quad (C10)$$

where (for $\hat{x} < d_1(t)$)

$$\hat{p}_0(\hat{x}, f(d_0) - t, t) = \frac{(2d_0)^{1/2} \dot{d}_0}{2(d_1 - \hat{x})^{1/2}}, \quad \hat{p}_1(\hat{x}, f(d_0) - t, t) = 0, \quad (C11)$$

it follows that

$$F_{II}(t) = \frac{\dot{d}_0 (2d_0)^{1/2}}{\epsilon^2} ((\delta_1 + \epsilon d_1)^{1/2} - \delta_2^{1/2}) + o(\epsilon^{-3/2} \delta_1). \quad (C12)$$

In the inner region III, $p^* = \epsilon^{-2} P_0 + o(\epsilon^{-2})$, where P_0 is given in terms of the leading-order inner potential Φ_0 in figure 8 by

$$P_0 = \frac{1}{2} \left(d_0^2 - \left(\frac{\partial \Phi_0}{\partial X} \right)^2 + \left(\frac{\partial \Phi_0}{\partial Y} \right)^2 \right). \quad (C13)$$

At leading order the pressure on the impactor is given by (for $-\infty < X < \infty$)

$$p^*(x^*, (f(\epsilon x) - t), t) = \epsilon^{-2} P_0(X, f'(d_0) d_1, t) + o(1), \quad (C14)$$

where (for $\xi > 0$)

$$P_0(X, f'(d_0) d_1, t) = \frac{\dot{d}_0^2}{2} \left(1 - \left(\frac{1 - \xi^{1/2}}{1 + \xi^{1/2}} \right)^2 \right), \quad X(\xi) = d_2 - \frac{H_J}{\pi} (1 + \xi + 4\xi^{1/2} + \ln \xi).$$

Using the second of these expressions to change the integration variable in $F_{III}(t)$ from X to ξ implies that

$$F_{III}(t) = -\frac{4d_0^2 H_J}{\epsilon \pi} \int_{\xi_-}^{\xi_+} \frac{d\xi}{\xi^{1/2}} + o(\epsilon^{-1}), \quad (C 15)$$

where ξ_{\pm} are the roots of $X(\xi_{\pm}) = \pm \delta_2/\epsilon^2$, so that, as $\delta_2/\epsilon^2 \rightarrow \infty$,

$$\xi_-^{1/2} = \left(\frac{\delta_2 \pi}{\epsilon^2 H_J} \right)^{1/2} - 2 + o(1) \quad (C 16)$$

while $\xi_+^{1/2}$ is exponentially small. Hence, the leading-order contribution to the force on the impactor from the jet-root region is given by

$$F_{III}(t) = \frac{8d_0^2 H_J}{\epsilon} \left(\frac{\delta_2 \pi}{\epsilon^2 H_J} \right)^{1/2} - \frac{16d_0^2 H_J}{\epsilon \pi} + o(\epsilon^{-1}); \quad (C 17)$$

the term of order $1/\epsilon$ in this expression is in agreement with the analysis of Korobkin (2006).

Finally, as described in Howison *et al.* (1991), the pressure on the impactor in the splash jets is of $O(\epsilon)$ and given in terms of the variables introduced at the end of §3 by

$$p^*(x^*, f(\epsilon x^*) - t, t) = -\epsilon f''(s) \eta_0(s, t) u_0(s, t)^2 + o(\epsilon), \quad (C 18)$$

so that

$$F_{IV}(t) = O(1). \quad (C 19)$$

Expanding (C 8) and (C 12), with $\epsilon^2 \ll \delta_2 \ll \epsilon \ll \delta_1 \ll 1$, and summing the contributions from (C 8), (C 12), (C 17) and (C 19) implies that the upward force on the impactor is given by (5.1), where $F_0 = \pi d_0 \dot{d}_0$ and

$$F_1 = \lim_{\delta_1 \downarrow 0} \left[\frac{(2d_0)^{1/2} \dot{d}_0 d_1}{\delta_1^{1/2}} + \frac{d_0}{2} \ln \left(\frac{\delta_1}{2d_0} \right) - 2 \int_0^{d_0 - \delta_1} \frac{\partial \phi_1}{\partial t}(x, 0, t) dx - 2d_0 \right]. \quad (C 20)$$

The local expansion (4.18) guarantees the existence of the limit in (C 20), with the first of these expressions allowing the second one to be written in the form (5.3).

REFERENCES

- CAMPBELL, I. M. C. & WEYNBERG, P. A. 1980 Measurements of parameters affecting slamming. *Rep.* 440, Wolfson Unit of Marine Technology, Tech. Rep. Centre No. OT-R-8042, Southampton, UK.
- COINTE, R. 1989 Two-dimensional water-solid impact. *Trans. ASME: J. Offshore Mech. Arc. Engng* **111**, 109–114.
- COINTE, R. & ARMAND, J.-L. 1987 Hydrodynamic impact analysis of a cylinder. *Trans. ASME: J. Offshore Mech. Arc. Engng* **109**, 237–243.
- DOBROVOL'SKAYA, Z. N. 1969 On some problems of similarity flow of fluid with a free surface. *J. Fluid Mech.* **36**, 805–829.
- FALTINSEN, O. M. 1990 *Sea Loads on Ships and Offshore Structures*. Cambridge University Press.
- FALTINSEN, O. M. 2002 On the entry of a wedge with finite deadrise angle. *J. Ship Res.* **46**, 39–51.
- FONTAINE, E. & COINTE, R. 1998 Asymptotic theories of incompressible water entry. *NASA* no.19980020557, France.
- FRAENKEL, L. E. & KEADY, G. 2004 On the entry of a wedge into water: the thin wedge and an all-purpose boundary layer equation. *J. Engng Maths* **48**, 219–252.
- FRAENKEL, L. E. & MCLEOD, J. B. 1997 Some results for the entry of a wedge into water. *Phil. Trans. R. Soc. Lond. A* **355**, 523–535.

- GAKHOV, F. D. 1966 *Boundary Value Problems*. Dover.
- GREENHOW, M. 1987 Wedge entry into initially calm water. *Appl. Ocean Res.* **9**, 214–223.
- HOWISON, S. D., OCKENDON, J. R. & OLIVER, J. M. 2002 Deep- and shallow-water slamming at small and zero deadrise angles. *J. Engng Maths* **42**, 373–388.
- HOWISON, S. D., OCKENDON, J. R. & OLIVER, J. M. 2004 Oblique slamming, planing and skimming. *J. Engng Maths* **48**, 321–337.
- HOWISON, S. D., OCKENDON, J. R., OLIVER, J. M., PURVIS, R. & SMITH, F. T. 2005 Droplet impact on a thin fluid layer. *J. Fluid Mech.* **542**, 1–23.
- HOWISON, S. D., OCKENDON, J. R. & WILSON, S. K. 1991 Incompressible water-entry problems at small deadrise angles. *J. Fluid Mech.* **222**, 215–230.
- VON KÁRMÁN, T. 1929 The impact of seaplane floats during landing. *NACA TN* 321, October, Washington.
- KOROBKIN, A. A. 1982 Formulation of the penetration problem as a variational inequality. *Din. Sploshnoi Sredy* **58**, 73–79.
- KOROBKIN, A. A. 1996 Water impact problems in ship hydrodynamics. *Adv. Mar. Hydrodyn.* **5**, 323–371.
- KOROBKIN, A. A. 2004 Analytical models of water impact. *Eur. J. App. Maths* **15**, 821–838.
- KOROBKIN, A. A. 2006 Second-order Wagner theory of wave impact. *J. Engng Maths* (submitted).
- KOROBKIN, A. A. & PUKHNACHOV, V. V. 1988 Initial stage of water impact. *Annu Rev. Fluid Mech.* **20**, 159–185.
- KOROBKIN, A. A. & SCOLAN, Y.-M. 2006 Three-dimensional theory of water impact. Part 2. Linearized Wagner problem. *J. Fluid Mech.* **549**, 343–373.
- LOGVINOVICH, G. V. 1996 *Hydrodynamics of Flows with Free Boundaries*. Naukova Dumka.
- MEI, X., LIU, Y. & YUE, D. K. P. 1999 On water impact of general two-dimensional sections. *Appl. Ocean Res.* **21**, 1–15.
- MIZOGUCHI, A. & TANIZAWA, K. 1996 Impact wave loads due to slamming – a review. *Ship Tech. Res.* **43**, 139–151.
- OLIVER, J. M. 2002 Water entry and related problems. DPhil thesis, University of Oxford.
- SCOLAN, Y.-M. & KOROBKIN, A. A. 2001 Three-dimensional theory of water impact. Part 1. Inverse Wagner problem. *J. Fluid Mech.* **440**, 293–326.
- VANDEN-BROECK, J.-M. & KELLER, J. B. 1993 Pouring flows with separation. *Phys. Fluids* A1, 156–159.
- VORUS, W. S. 1996 A flat cylinder theory for vessel impact and steady planing resistance. *J. Ship Res.* **40**, 89–106.
- WAGNER, H. 1932 Über stoß- und gleitvorgänge an der oberfläche von flüssigkeiten (Phenomena associated with impacts and sliding on liquid surfaces). *Z. Angew. Math. Mech.* **12**, 193–215.
- WILSON, S. K. 1989 The mathematics of ship slamming. DPhil thesis, University of Oxford.
- ZHAO, R. & FALTINSEN, O. 1993 Water-entry of two-dimensional bodies. *J. Fluid Mech.* **246**, 593–212.
- ZHAO, R., FALTINSEN, O. & AARSNES, J. 1996 Water entry of arbitrary two-dimensional sections with and without separation. *Proc. 21st Symposium on Naval Hydrodynamics*, pp. 118–133, Trondheim, Norway.